IEEE Access
Multidisciplinary | Rapid Review | Open Access Journal

Received February 25, 2021, accepted February 26, 2021, date of publication March 8, 2021, date of current version March 15, 2021.

Digital Object Identifier 10.1109/ACCESS.2021.3064206

Galvanic Impulse Wireless Communication for Biomedical Implants

REZA NOORMOHAMMADI[1], ALI KHALEGHI[1,2], (Senior Member, IEEE), AND ILANGKO BALASINGHAM[1,2], (Senior Member, IEEE)

[1]Department of Electronic Systems, Norwegian University of Science and Technology, 7491 Trondheim, Norway
[2]Intervention Center, Oslo University Hospital, 0027 Oslo, Norway

Corresponding author: Reza Noormohammadi (reza.noormohammadi@ntnu.no)

This work was supported by the Research Council of Norway through the Wireless In-body Sensor and Actuator Networks (WINNOW) Project under Grant 270957.

ABSTRACT Wireless intra-body communication is a promising approach for providing efficient and secure connectivity for medical implants. The low power consumption of the electronics and the conductivity of the biological tissues facilitate the system implementation, which makes the technique more power-efficient than the traditional radio frequency wireless systems. The galvanic intra-body communication uses the electrical current for signal transmission in the conductive medium of the biological tissues. In this paper, we propose an ultra-low-power communication approach by implementing a galvanic impulse method for communication between an implant and an on-body device. The communication system is designed, manufactured with off-the-shelf electronic components, and measured in the phantom and in-vivo animal experiment. The implant power consumption is 45 μW for the data rate of 64 kbps with a bit error percentage below 0.5% for the implant depth of 14 cm. The design supports long-lasting battery-powered implant sensory and communication system.

INDEX TERMS Galvanic coupling, intra-body communication, biomedical implants, biomedical electronics, ultra-wideband.

I. INTRODUCTION

Wireless health-care monitoring is an emerging technology that overcomes the limitations of conventional clinical methods. The main advantage is long term and continuous monitoring of the patients with the possibility of data mining for applying machine learning methods for improved medical advice for a higher quality of life. Implantable devices play a crucial rule in the technology development that can have sensors with the possibility of collecting internal body information for an organ-specific diagnostic purpose. Data communication plays a key role in system development, where wireless connectivity between an implant and the external body is a requirement. Implementing wireless communication technology for long-lasting medical implants is vital, because of significant limitations imposed by using a wire-based system, in which the wire is the source of infections and has limitations by passing through the biological organs. Still, there are several technical challenges in developing reliable and ultra-low-power wireless implantable devices, especially for the deep implants in which it would be difficult to change the implant energy sources like the battery. Using conventional radio frequency (RF) for implant wireless communication is not power-efficient. This can significantly influence the life span of a wireless implant. The main reason for the high-power requirement for an RF system is the power hungry local oscillators and accurate clock production and recovery system that lead to complex and high power demand design. This is in addition to the significant attenuation of the RF signal by transmission through the body tissues. Also, the small available size for the RF antenna reduces the radiation efficiency of the antenna, and the antenna integration with the implant casing is usually problematic, especially for the implants with metal casing. The main advantage of using RF is the high available bandwidth that can support a high data rate, while most implant sensors require low data rate [1], except in some visual inspections in which a high data rate sensor is involved such as video capsule endoscopy [2] or neural implants for recording brain signals. As an example, electrocardiogram (ECG) requires about 72 kbps for

The associate editor coordinating the review of this manuscript and approving it for publication was Cihun-Siyong Gong.

a sampling frequency of 500 Hz, resolution 12 bit, and 12 recording channels [3].

Table 1 summarizes several states of the art communication technologies used for implants. An implantable transceiver operating at 396 - 447 MHz has been proposed in [4], in which a loop antenna is used for the transmission, the power consumption for a data rate of 25 kbps is 2.2 mW using OOK modulation for implant depth of 8 cm. Ultra-wideband (UWB) signaling in GHz band is considered as a low power approach because the active duty cycle in comparison to the bit duration is very low. This leads to having total power consumption less than the narrow band RF links [5]. In [6] a full-duplex UWB transceiver is proposed for the neural interface in which an impulse radio (IR) UWB link has been used to support the in-body to on-body communication. The total power consumption for a data rate of 500 Mbps with OOK modulation is 5.1 mW. It should be noticed that the proposed system is applied for the subcutaneous implants. To support deep implant communication using UWB at GHz frequencies, the transmitter power should be increased dramatically because of the high signal attenuation in biological tissues in GHz band. In [7], an inductive coupling based transceiver for neural implants has been proposed. The final on-chip prototype has been tested on an animal skull and has achieved a 200 Mb/s data rate for the implant depth of 11.8 mm with 300 μW total power consumption.

TABLE 1. Performance comparison of different implants communication.

	Power consumption	Frequency	Data rate	Implant depth
RF Narrow Band[4]	2.2 mW	396-447 MHz	25 kbps	8 cm
Inductive Coupling [7]	300 μW	200 MHz (Carrier)	200 Mbps	1.18 cm
IR-UWB [6]	5.1 mW	3.1-7 GHz	500 Mbps	-
Capacitive IBC [9]	-	1 MHz (Carrier)	170 kbps	1 cm
Galvanic Coupling [12]	3.7 mW	32 MHz (Carrier)	6 Mbps	11 cm
This work	45 μW	0.01-10 MHz	64 kbps	14 cm

Capacitive coupling, galvanic coupling, and magnetic coupling are the recent approaches to overcome the power consumption limitations associated using RF and UWB [8]. In capacitive coupling, the signal propagates through the body by using an electric field induced by a pair of electrodes to the body. As a realized transceiver, in [9], a capacitive coupling based link has been proposed for both power and data delivery. The data rate of 170 kbps has been achieved at a maximum distance of 10 mm by using the delivered power of 12 mW to the load. The exact power consumption value for the data link is not available in [9]. The advantage of power delivery by using capacitive coupling over inductive coupling is its less sensitivity to tissue contact and carrier frequency variation due to its high pass nature.

In magnetic coupling, the approach is similar to the inductive coupling method in which the produced magnetic field by a coil passes through the body and can be received by another coil. The main advantage of this method is lower path loss in comparison to the other methods, and this is due to the fact that the body tissues are lossless for the magnetic field [10].

In galvanic coupling, a weak electric current is injected into the tissue, and by modulating this electric current, the desired signal is transmitted toward another implant [11]. In [12], an IBC transmitter based on galvanic coupling for digital capsule endoscopy has been proposed. The final prototype has 6 Mbps data rate with overall power consumption of 3.7 mW in the link distance of 11 cm.

In Table 1 overall performance of the reviewed methods has been compared in terms of power consumption, data rate, frequency band, and implant depth. Regarding the comparison between the methods and current state of the art works and comprehensive study on intra-body communications [13], the galvanic coupling is a promising method of communication for deep implants because of the following reasons:

- Low path loss: due to the conductive nature of the body tissues applying an electric current signal is preferable to the electric field for communication.
- Less complexity in circuits: due to the good performance of galvanic communication in sub MHz frequencies, the circuit design is simpler because there is no need to have complex blocks like accurate clock generators and synchronizer.
- Low power consumption: due to the low path loss and low-frequency operation of the galvanic links, the overall power consumption is potentially less than the other methods.

By considering these facts, a low power galvanic impulse link is proposed for intra-body communication. The main contribution of the paper is the novel impulse generator circuit which is more power-efficient than conventional impulse generators. The rest of the paper is organized as follows: In Section II the electromagnetic simulation scenarios are defined, in Section III the transmitter electronic circuit is presented in detail, in Section IV the receiver system and setup for data demodulation and detection are discussed, in Section V the phantom and in-vivo animal experiments are conducted, and the measurement results are presented. Section VI concludes the paper.

II. NUMERICAL ELECTRODES SIMULATIONS

In galvanic coupling, the signal transmission is based on electrical current flow in the medium. So the medium's conductivity is a key factor in galvanic coupling because it determines the ability of the medium to allow electrical current flow. The electrode impedance of a galvanic link can change in a wide range because it is directly related to the medium's conductivity. So, simulating the electrode antennas in the body tissues model for having an approximate value for impedance and link loss is essential. For our work, the in-body electrode consists of two metal plates separated with a given distance. The electrode impedance is a complex value

and depends on the frequency of operation, electrode geometry, and the involved tissues. By having a larger electrode size, the real part of the impedance reduces because of having better contact with the medium.

The frequency band for electrode impedance simulation is in the range 1-5 MHz. The bandwidth for communication is within the range of 10 kHz to 10 MHz. The lower edge is limited by balun used in phantom and in-vivo measurements. The upper edge is selected based on the impulse signal spectrum produced at the transmitter side.

Gabriel material properties data [14] is used to characterize the biological environment. In Gabriel's measurements, the dielectric properties of the human body tissues have been measured in a wide frequency range from 10 Hz to 20 GHz over 20 different tissue types. The numerical computation model is implemented to characterize the electrodes and the communication channel using full-wave electromagnetic simulation in CST Microwave Studio. We use both finite element frequency domain (FEM) and finite difference time domain (FDTD) solvers for verifying the accuracy of computations. Because of the low-frequency operation of the link, the wavelength is much higher than the tissue size, so no need to consider the radiation parameter for the boundary. So we considered an open boundary with an air gap of 1 cm around the simulation model. In Fig. 1, the simulation scenarios in the homogeneous muscle tissue have been depicted. The location of the on-body antenna is fixed, but the transmitter implant location varies for observing the link gain (path-loss) for different distances, orientations, and sizes.

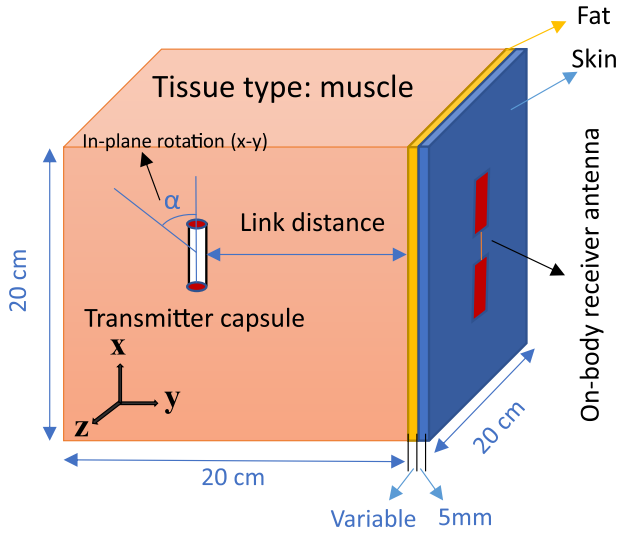

FIGURE 1. Transmitter capsule inside the homogeneous muscle tissue. Receiver patch antenna with two square shape electrodes (20 mm×20 mm), and separation (120 mm) in contact with the multilayer (skin-fat-muscle) model.

The capsule is simulated as an air-filled cylinder with two metal electrodes of diameter = 7 mm and thickness = 0.1 mm with the capsule length of 40 mm (Fig. 2-a). The electrodes are in direct contact with the biological tissues. Since the electric current diminishes significantly with distance to the

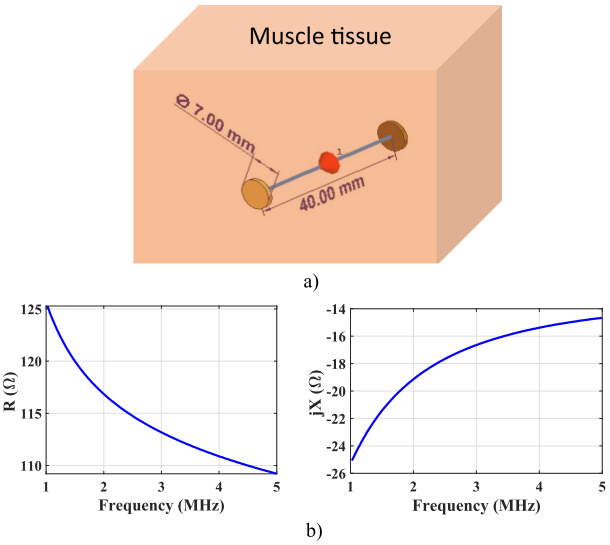

FIGURE 2. a) The capsule electrodes geometry for the simulation inside homogeneous tissue model, L = 40 mm, electrode diameter 7 mm, thickness = 0.1 mm b) real and imaginary part of the electrodes impedance inside the muscle tissue versus frequency are depicted.

capsule, the selected tissue size is enough to simulate the capsule impedance and coupling link parameters. Adding the tissue size increase the simulation time and memory, and slight changes in the simulation parameters can be observed. In Fig. 2-b, the capsule impedance inside the medium is depicted.

The on-body antenna considered as two square patches with 20 mm × 20 mm size and 120 mm distance between the electrodes (Fig. 3-a). The impedance of the on-body antenna is shown in Fig. 3-b. The resistive part of the on-body antenna impedance is almost half of the capsule electrodes.

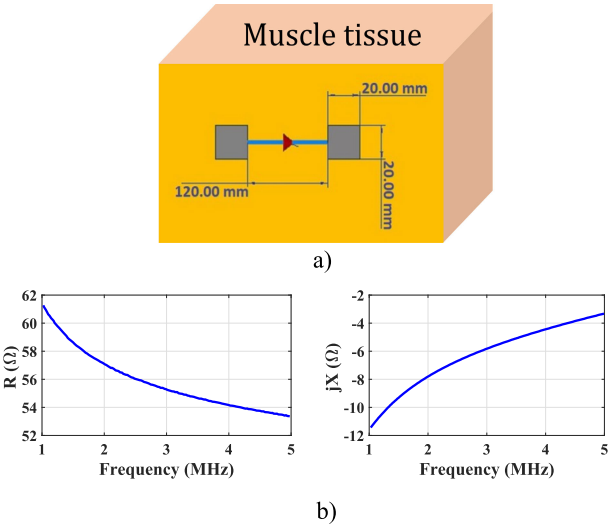

FIGURE 3. a) On-body antenna simulation model which is considered as two conductive patches, patch sizes (20 *mm* × 20 *mm*), separation distance 120 mm, b) real and imaginary part of the impedance for on-body patch antenna in the frequency range of 1 MHz to 5 MHz.

The main reason is the higher contact area of the on-body patch antenna with the biological tissue than the capsule electrodes. By increasing the contact area, the resistance of the electrodes will reduce gradually. Here, the impedance is about 50 Ω, which is a good solution for operating with standard source impedance if applied. It must be mentioned that based on the simulation, mutual impedance of the antennas has negligible effect on the self-impedance of both implant and on-body antennas.

The channel gain simulation versus link distance is depicted in Fig. 4, in which the channel gain is defined as $20log_{10}(V_{peakRX}/V_{peakTX})$. Figure 4-a shows the channel gain in a homogeneous muscle medium versus distance between implant and on-body antenna. As shown in Fig.4-a, by increasing the separation distance between the implant and on-body receiver ($d > 20mm$), the path loss increases with a linear rate (2 dB/cm), and for larger distances the reduction rate is reduced to about (1 dB/cm). For considering the multilayer tissue effect, skin and fat layers are added in the channel modelling. The addition of a skin layer of thickness 5 mm, has very small influence in the channel gain; by including a fat layer under the skin, the coupling reduces significantly. Figure 4-b shows the channel gain at a nominal depth of 100 mm versus the fat thickness below the skin (see Fig. 1). As shown, by adding the fat layer a sharp drop in the channel gain is observed, and then the gain reduction with the addition of fat thickness becomes marginal.

In conclusion, because of the electrical current based nature of the galvanic coupling, the best path from transmitter to the receiver is not necessarily the geometrical shortest path, especially for the heterogeneous tissues in which multiple tissue properties may be involved. In fact, the current path finds the lowest resistance path to the receiver. In other words, the applied voltage to the transmitter electrodes produce a current in the medium, and this current tends to flow from a path with the lowest electric resistance mostly. So, depending on the location of the transmitter and receiver electrodes, the path loss and also the impedance of the medium can vary. The effect of electrode rotation and capsule length on the path loss inside muscle tissue is depicted in Fig. 5. The distance between the transmitter capsule and receiver is fixed at 100 mm (see Fig. 1 for rotation definition and antenna placement). According to the results, the capsule rotation in the worst case can increase the path loss to -110 dB in 90-degree rotation from the reference angle. Also, the capsule length has a direct impact on channel gain as it could be anticipated because by increasing the capsule length, the electric current lines between the electrodes will have a longer path so that they can penetrate larger distance. Figure 5-c shows the effect of displacement relative to the on-body antenna in lateral and longitude, z- and x-, directions on the channel gain. As shown, in the lateral displacement the gain variation is less than the longitude displacement due to the nature of the placement of the on-body electrodes. Figure 6 shows the simulated electric field intensity for the capsule and the on-body antenna at 3 MHz frequency in the muscle tissue. According

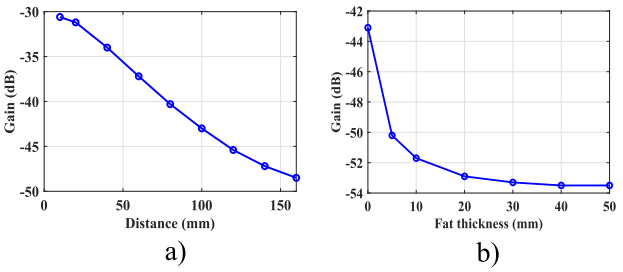

FIGURE 4. a) Channel gain versus distance for capsule (length 40mm, electrode diameter 7mm), in parallel with the on-body electrode receiver (patch sizes 20mm×20mm, separation 120mm), without lateral and longitude displacement in the muscle model b) Channel gain at a depth of 100 mm for skin thickness 5 mm, and variable fat thickness.

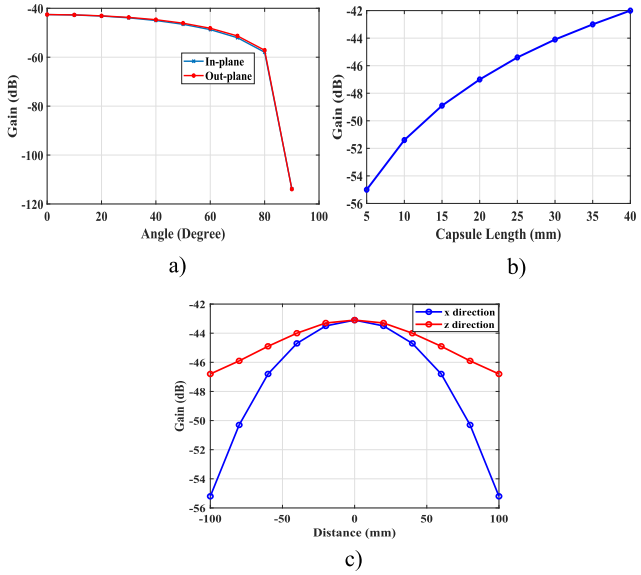

FIGURE 5. a) Effect of the capsule rotation on channel gain and, b) effect of the capsule electrodes length with fixed capsule angle ($\alpha = 0$) on the channel gain at 10 cm depth, c) channel gain inside homogeneous muscle tissue, versus lateral (z-direction) and longitude (x-direction) displacements within the depth of 10 cm. See Fig. 1 for capsule and on-body antenna positions.

to the electric field distribution around the on-body antenna, by having larger electrode separation, the coverage area will be increased, but the coverage underneath of the central feed point will be reduced. A compromise between the coverage area, gain, and depth should be considered.

III. TRANSMITTER SETUP AND ELECTRONICS

To realize a galvanic coupling based deep implant communication the operating frequency for best performance in terms of path loss regarding the different electrodes size and distance is from around 10s of kHz to 30 MHz [8], [15], [16]. Another advantage of using rather low operating frequency is its lower power consumption and less complex circuits for signal generation. Also due to the very long wavelength in this frequency range, the radiation of the signal in the environment is very low which makes it difficult to sniff the signal from distance, so it is more secure than RF signals which naturally have sensible radiation because of their

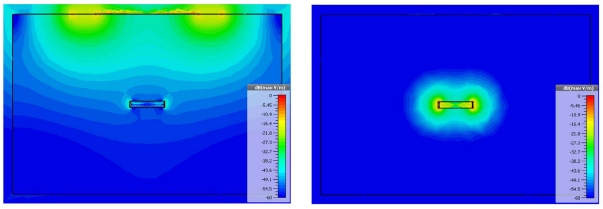

FIGURE 6. Electric field intensity in the cut plane of antennas in the muscle tissue by applying an electric voltage difference between the electrodes at 3 MHz frequency, a) on-body patch excitation b) implant electrode excitation.

shorter wavelength [17]. The designed data rate for the link is 64 kbps. Also, in order to make the transmitter more power efficient, we have used baseband impulse technique for the transmitter signal generation; therefore, as fast electronics are not required, which can save the system power consumption. By using the impulse shape for the signal, we have a very short active duty cycle around 20 ns for 3 dB amplitude reduction. In comparison to the bit duration of 15.6 μs (for 64 kbps data rate), the power consumption reduces by a factor of 780 compared to a continuous transmission method with the same signal amplitude ($P_{Cont.}/P_{Impulse} = 15.6\ \mu s/20ns = 780$). It must be mentioned that we achieve this power reduction for the price of having higher bandwidth [18]; however, the on-body receiver system has fewer limitations with power that can compensate for the system performance degradation due to increased bandwidth. Also, due to the low frequency operation of the link, we have not used carrier frequency for the signal, which makes it more power-efficient. Figure 7 shows the block diagram of the transmitter.

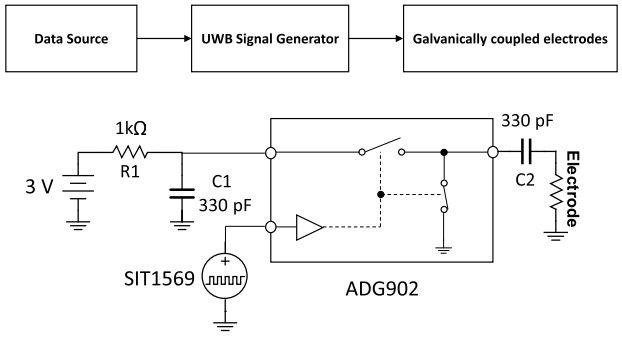

FIGURE 7. Transmitter block diagram and schematic. The capsule electrodes considered as resistive load for the transmitter circuit.

For impulse signal generation, we use two high-speed switches [19] that connect a charged 330 pF capacitor to the channel. For controlling the pulse duration, we can change the value of the capacitor C1. The resistor R1 is for controlling the charge time constant of the capacitor C1. The capacitor C2 is for removing DC component of the generated signal. The advantage of using the mentioned method for impulse signal generation is its higher power conversion efficiency from power supply to injected energy in the channel. The power consumption of the high-speed switch is in the order of 0.1 μA for 3 V power supply [19]. The popular method for producing impulse signal is by using digital *AND* gates, in which one of the inputs is connected to the data source, and another branch is connected with a delayed version of data by digital buffer gates [20]. By using the number of buffer gates, we can control the delay value and pulse width. By changing the number of buffer gates for the desired delay, the efficiency of the circuit reduces due to the power consumption of the gates. Also in narrowband transmitters which are mainly based on local oscillator blocks, the oscillators usually have the efficiency of less than 50 percent, and for the output stability, there is usually a buffer amplifier needed to isolate the oscillator output from next stages to make it more stable in terms of frequency and amplitude fluctuations which in general decreases the power efficiency [21]. However, in the proposed method, the pulse duration can be changed by changing the capacitor value. Also, the stored energy in the capacitor is discharged in the environment without any extra loss, which could have power coupling efficiency close to 100 percent depending on the capacitor quality factor.

In Fig. 8 the time domain waveform and frequency spectrum of the produced pulse are shown. As can be seen, the pulse duration is in order of 20 ns, that is much smaller than a bit duration for 64 Kbps. We note that 20 ns pulse duration depends on the discharge time of the capacitor, and the discharge time constant depends on the electrode impedance, which is directly related to the type of the body tissue. So, for the tissues with less conductivity, we will have larger impedance for the capsule and then higher discharge time and higher bit duration. Therefore, for having a specific value for the bit duration, the capsule electrodes should be designed in a way that the impedance meets the required value for discharge time constant. For this aim, we considered the capsule electrode size and capacitors values to have the real impedance value to meet the required pulse duration. The second capacitor, which is in series with the electrode is for having a negative peak signal for the ''0'' bit transmission. In Fig. 9 the final prototype of the transmitter capsule is depicted.

IV. RECEIVER STRUCTURE AND PERFORMANCE

On the receiver side, a balun has been used for isolating the antenna from the receiver setup and rejecting the common mode interference signal [22], then a low-pass filter is applied to reject the out of band interference signals. The overall effect appears as a bandpass filter. Figure 10 shows the block diagram of the receiver. For the detection and data processing purpose, the received signal is sampled using a digital sampling oscilloscope (HMO2024), the recorded signal is used in off-line processing by GNURadio platform for data detection and bit error rate (BER) calculations. A threshold-based data detection is used for data decoding with a positive threshold for bit "1" and a negative threshold for bit "0". For having a reliable threshold value for different link distances, a digital

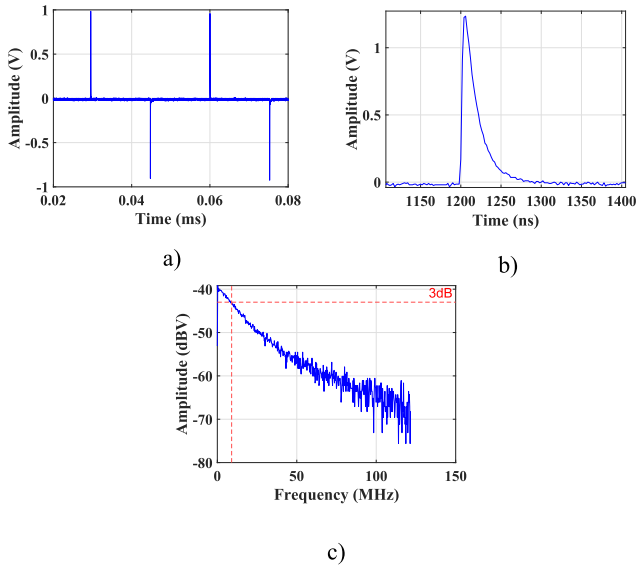

FIGURE 8. (a) Time domain signal of the transmitter on 50 Ω resistive load, (b) single pulse shape measured on the 50 Ω load, and (c) frequency spectrum of transmitter output with 50 Ω load. The 3dB bandwidth of the signal is 10 MHz.

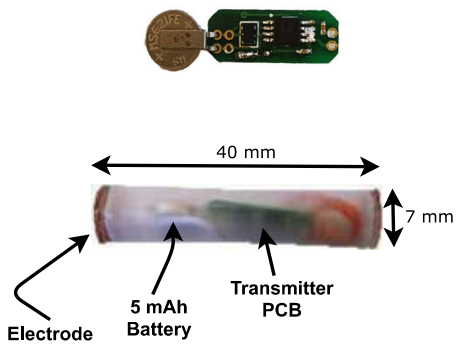

FIGURE 9. Transmitter circuit enclosed in a 3D-printed capsule shell. The electrodes are placed at two ends of the capsule shell.

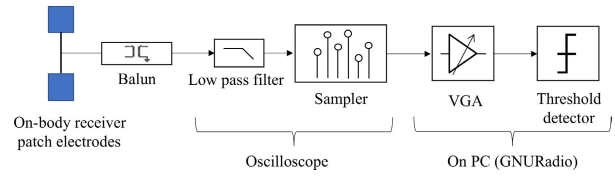

FIGURE 10. Receiver block diagram.

variable gain amplifier (VGA) is used before applying the thresholder.

The simulation for the BER has been done by using GNURadio platform. For this aim, the transmitter output signal for "0" and "1" is sampled and recorded. Then in the GNURadio platform, the recorded file is used to model the transmitter output. For simulating the channel, we assume additive white Gaussian noise (AWGN) channel in which is a valid assumption for the galvanic coupling in the given operating frequency [23]. Besides, we assume that the channel is stationary during the signal transmission [23]. By adding the produced noise to the received signal, we simulate the real link, and then by applying the threshold detection method to the noisy signal, we obtain BER for different signal to noise (SNR) values. The bit stress pattern for the BER simulation is alternating "0" and "1" and the observation window size is 30 Mb. The BER simulation procedure is shown in Fig. 11-a and the BER simulation result is shown in Fig. 11-b.

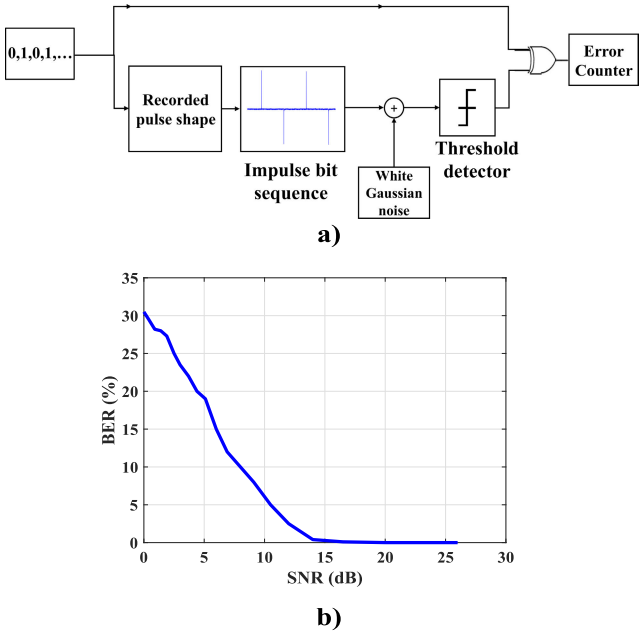

FIGURE 11. (a) Block diagram of the BER simulation, (b) simulated BER in AWGN channel for different SNR values. The simulation was conducted in GNURadio platform.

V. MEASUREMENT SETUP AND RESULTS

For testing the proposed design, a liquid phantom is prepared in a way that simulates the homogeneous muscle tissue used in the simulation. In Fig. 12-a the block diagram of the measurement setup, and in Fig. 12-b the laboratory setup for the liquid phantom is depicted. The liquid phantom is prepared using aqua based saline solution in which the sea salt (NaCl) volume concentration of 0.14% can provide similar material properties to the muscle data from Gabriel model [14] at 3 MHz with 10% material property variation in the wide frequency range of 1-5 MHz. Also, an animal experiment (in-vivo test) has been done to evaluate the link performance in inhomogeneous (multilayer) area. The in-vivo experiment was done at the Intervention Centre of Oslo University Hospital, Oslo, Norway. The experiment was carried out under strict clinical standards regarding the ethical and humane treatment of animals, and the animal was under a general anesthetic during the trial.

In Fig. 13, the block diagram and photograph of the in-vivo test and clinical environment are shown. The on-body patch antenna is the same as the simulated antenna in Section II Fig. 3-a. The transmitter capsule was placed in the abdominal

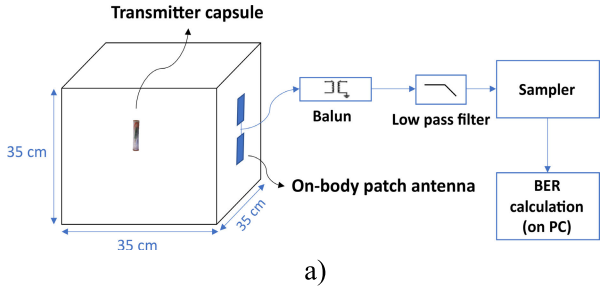

a)

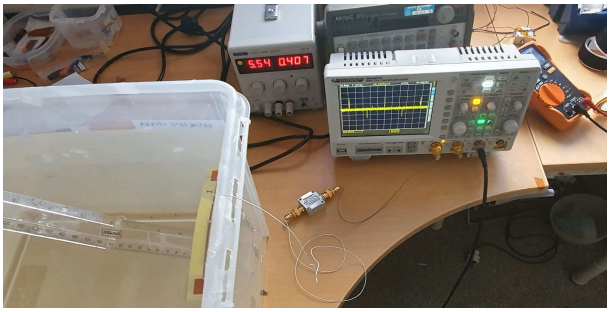

b)

FIGURE 12. a) Block diagram of the phantom setup for in-body to on-body communication, b) phantom measurement in the lab environment. The transmitter capsule is connected to a holder for accurate link distance measurement and the on-body antenna is fixed in a way that it has direct contact with the liquid phantom.

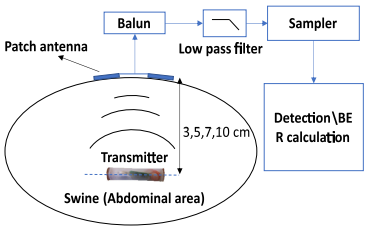

a)

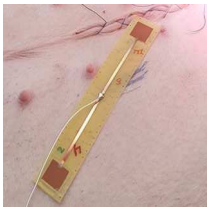

b)

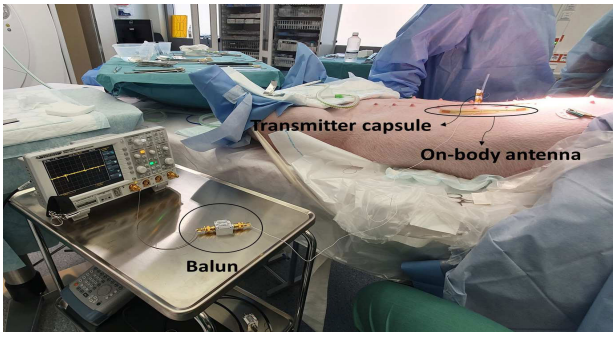

c)

FIGURE 13. a) System block diagram used in the in-vivo setup, b) on-body patch antenna placed on top of the abdominal area. c) The animal experiment setup. Transmitter capsule is attached to a holder and placed in the abdominal area. After placing the transmitter capsule, the cut was firmly closed so that the transmitter implant was in a realistic situation.

area of the swine. We selected the abdominal area because of its simplicity of surgery. During the animal experiment, it is needed to open the cut and check the capsule's position and distance several times. For opening and closing the cut easily abdominal area was the best option. Other places like the chest have difficulty of surgery as it is needed to cut the ribs. Also, there is a lot of uncertainty in the distance and the communication channel itself when the implant is under the chest because of the lungs and breathing. For controlling the implant depth and alignment, the capsule was attached to a holder for controlling the capsule direction and distance from the on-body antenna. The on-body antenna was placed on the skin. We first tested dry contact between the on-body antenna and swine skin; the signal was close to the noise level. After applying the conductive saline gel to the antenna contact surface, the received signal improved by 12 dB. So the antenna contact quality needs to be considered as an important factor in the receiver side. For removing the common mode noise in the test, which is the main interference signals in low-frequency links, a balun (FTB-1-6+) has been used at the receiver part. The 3 dB cut-off frequency of the balun is 0.01 MHz and 125 MHz. In Fig. 14, the effect of using balun on a single pulse and received signal have been shown. It can be seen that without using balun, the interference level at the receiver is much higher than by using a balun. Also, in order to see the influence of the parasitic paths due to the metallic trolley under the balun in the in-vivo experiment (see Fig. 13-c), we repeated the phantom measurement with a metallic plate under the balun to mimic the in-vivo situation, and the channel gain in both phantom scenarios had less than 0.5 dB difference. Figure 15 shows the measured channel gain for the liquid phantom (homogeneous model), homogeneous simulation model (muscle), multi-layer simulation model

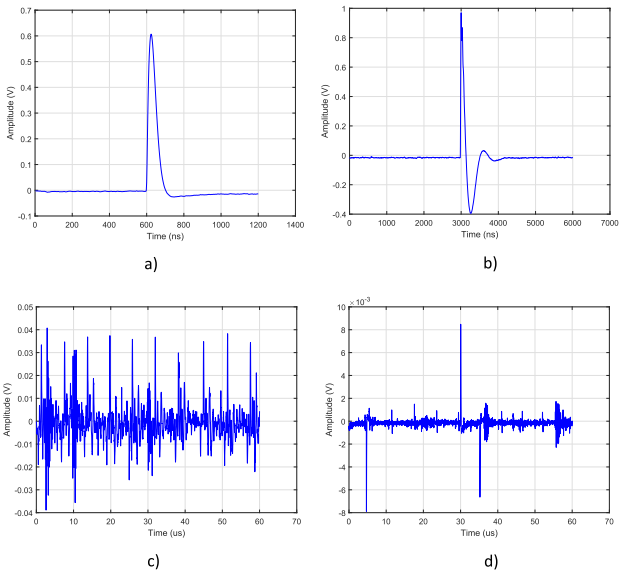

FIGURE 14. (a) Received signal without using balun when the transmitter is directly connected to the receiver with 50 Ω load, (b) effect of using balun on a single pulse at the receiver, (c) receiver without balun with 7 cm link distance. Low frequency interferences are picked up by the receiver without using the balun and reduce the signal to noise ratio, which leads to worse receiver performance, d) receiver with the balun.

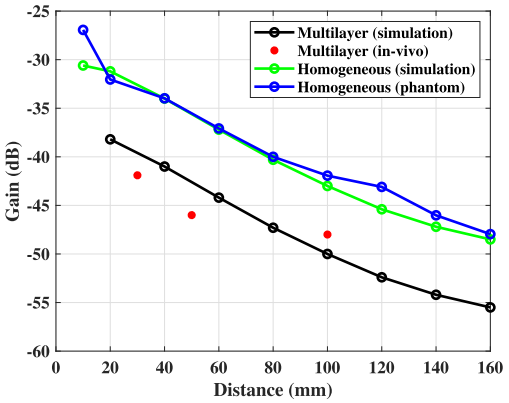

FIGURE 15. Channel gain versus capsule depth for in-vivo measurement and comparison with homogeneous and multilayer tissue simulation and liquid phantom measurement.

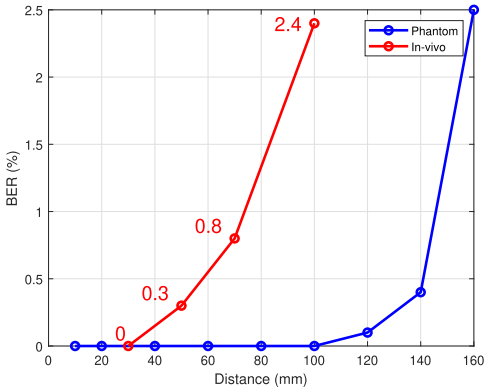

FIGURE 16. Measured BER results for in-vivo and phantom experiments for different depth values.

(skin = 5mm, fat = 5mm, muscle), and in-vivo measurement. For in-vivo measurement, the balun insertion loss and saline gel effect are taken into account. As shown, the results for in-vivo measurement and multilayer simulation are in close agreement. The phantom measurements are close to homogeneous simulation. The in-vivo measurement has about 10 dB higher loss than phantom measurement. This higher loss is due to the presence of fat and skin in the in-vivo test, especially for the fat, because the conductivity is less than other tissue types [14] and, it contributes to having more channel loss. In Fig. 16, the BER plot for the phantom setup and in-vivo setup is shown. As a consequence of having higher channel loss for multilayer environment (abdominal area), the BER value for the in-vivo test is higher than the homogeneous environment (phantom). Transmitted bit pattern for the BER measurement is alternating "0" and "1". The observation window for each BER point is 10 Kb. It must be noted that the BER results are for the link without using channel coding techniques. By using a channel coding, the BER performance could be improved depending on the coding algorithm, but with increased power consumption in the system.

VI. CONCLUSION

An ultra-low-power data telemetry for biomedical deep implants based on galvanic impulse is proposed. The transmitter uses carrier-less signaling that reduces the electronics power consumption. The total power consumption for the implant is 45 μW for data rate of 64 kbps. Galvanic current injection is used for inducing generated data signal to the medium that increases the link gain and coupling efficiency. The developed circuit was encapsulated into a small 7mm $\times$ 40mm cylindrical plastic capsule shell. The fabricated setup was tested inside liquid phantom as a homogeneous medium like muscle tissue. For heterogeneous medium, the setup was further tested inside the abdominal area of a living animal. The bit error rate results show that the proposed link has less than 0.5 % error for 14 cm distance in homogeneous medium and 10 cm distance with less than 2.5 % BER for multilayer and complex medium without channel coding techniques. As a summary, the galvanic impulse technique is a promising approach for intra-body communication because of its lower power consumption, less channel attenuation, and higher coupling efficiency combined with higher data security level.

ACKNOWLEDGMENT

The authors thank surgeon J. Bergsland, and the surgical team for performing the animal experiment at the Intervention Center, Oslo University Hospital.

REFERENCES

[1] J.-Y. Hsieh, Y.-C. Huang, P.-H. Kuo, T. Wang, and S.-S. Lu, "A 0.45-V low-power OOK/FSK RF receiver in 0.18 μm CMOS technology for implantable medical applications," *IEEE Trans. Circuits Syst. I, Reg. Papers*, vol. 63, no. 8, pp. 1123–1130, Aug. 2016.

[2] R. Noormohammadi, A. Khaleghi, and I. Balasingham, "Battery-free wireless communication for video capsule endoscopy," in *Proc. 13th Int. Symp. Med. Inf. Commun. Technol. (ISMICT)*, May 2019, pp. 1–5.

[3] J. Bae, K. Song, H. Lee, H. Cho, and H.-J. Yoo, "A low-energy crystal-less double-FSK sensor node transceiver for wireless body-area network," *IEEE J. Solid-State Circuits*, vol. 47, no. 11, pp. 2678–2692, Nov. 2012.

[4] S.-J. Yun, J. Lee, J. Kang, C. Bae, J. Suh, and S. J. Kim, "A low power fully intergrated RF transceiver for medical implant communication," in *Proc. IEEE Int. Symp. Circuits Syst. (ISCAS)*, May 2018, pp. 1–4.

[5] A. Ghildiyal, K. Amara, R. D. Molin, B. Godara, A. Amara, and R. K. Shevgaonkar, "UWB for in-body medical implants: A viable option," in *Proc. IEEE Int. Conf. Ultra-Wideband*, Sep. 2010, pp. 1–4.

[6] S. A. Mirbozorgi, H. Bahrami, M. Sawan, L. Rusch, and B. Gosselin, "A full-duplex wireless integrated transceiver for implant-to-air data communications," in *Proc. IEEE Custom Integr. Circuits Conf. (CICC)*, Sep. 2015, pp. 1–4.

[7] W. Li, Y. Duan, and J. Rabaey, "A 200-Mb/s energy efficient transcranial transmitter using inductive coupling," *IEEE Trans. Biomed. Circuits Syst.*, vol. 13, no. 2, pp. 435–443, Apr. 2019.

[8] M. Li, Y. Song, Y. Hou, N. Li, Y. Jiang, M. Sulaman, and Q. Hao, "Comparable investigation of characteristics for implant intra-body communication based on galvanic and capacitive coupling," *IEEE Trans. Biomed. Circuits Syst.*, vol. 13, no. 6, pp. 1747–1758, Dec. 2019.

[9] A. Koruprolu, S. Nag, R. Erfani, and P. Mohseni, "Capacitive wireless power and data transfer for implantable medical devices," in *Proc. IEEE Biomed. Circuits Syst. Conf. (BioCAS)*, Oct. 2018, pp. 1–4.

[10] H.-J. Kim, H. Hirayama, S. Kim, K. J. Han, R. Zhang, and J.-W. Choi, "Review of near-field wireless power and communication for biomedical applications," *IEEE Access*, vol. 5, pp. 21264–21285, 2017.

[11] M. S. Wegmueller, A. Kuhn, J. Froehlich, M. Oberle, N. Felber, N. Kuster, and W. Fichtner, "An attempt to model the human body as a communication channel," *IEEE Trans. Biomed. Eng.*, vol. 54, no. 10, pp. 1851–1857, Oct. 2007.
[12] M. Park, T. Kang, I. Lim, K.-I. Oh, S.-E. Kim, J.-J. Lee, and H.-I. Park, "Low-power, high data-rate digital capsule endoscopy using human body communication," *Appl. Sci.*, vol. 8, no. 9, p. 1414, Aug. 2018.
[13] W. J. Tomlinson, S. Banou, C. Yu, M. Stojanovic, and K. R. Chowdhury, "Comprehensive survey of galvanic coupling and alternative intra-body communication technologies," *IEEE Commun. Surveys Tuts.*, vol. 21, no. 2, pp. 1145–1164, 2nd Quart., 2019.
[14] S. Gabriel, R. W. Lau, and C. Gabriel, "The dielectric properties of biological tissues: II. Measurements in the frequency range 10 Hz to 20 GHz," *Phys. Med. Biol.*, vol. 41, no. 11, p. 2251, 1996.
[15] M. Swaminathan, F. S. Cabrera, J. S. Pujol, U. Muncuk, G. Schirner, and K. R. Chowdhury, "Multi-path model and sensitivity analysis for galvanic coupled intra-body communication through layered tissue," *IEEE Trans. Biomed. Circuits Syst.*, vol. 10, no. 2, pp. 339–351, Apr. 2016.
[16] A. K. Teshome, B. Kibret, and D. T. H. Lai, "Galvanically coupled intrabody communications for medical implants: A unified analytic model," *IEEE Trans. Antennas Propag.*, vol. 64, no. 7, pp. 2989–3002, Jul. 2016.
[17] M. Maldari, M. Albatat, J. Bergsland, Y. Haddab, C. Jabbour, and P. Desgreys, "Wide frequency characterization of intra-body communication for leadless pacemakers," *IEEE Trans. Biomed. Eng.*, vol. 67, no. 11, pp. 3223–3233, Nov. 2020.
[18] L. Yang and G. B. Giannakis, "Ultra-wideband communications: An idea whose time has come," *IEEE Signal Process. Mag.*, vol. 21, no. 6, pp. 26–54, Nov. 2004.
[19] *ADG902 High-Speed SPST Switches*, Analog Devices, Norwood, MA, USA, 2017.
[20] S. Schmickl, T. Faseth, and H. Pretl, "An RF-energy harvester and IR-UWB transmitter for ultra-low-power battery-less biosensors," *IEEE Trans. Circuits Syst. I, Reg. Papers*, vol. 67, no. 5, pp. 1–10, May 2020.
[21] P. Kinget, "Integrated GHz voltage controlled oscillators," in *Analog Circuit Design*. Boston, MA, USA: Springer, 1999, pp. 353–381.
[22] M. A. Callejon, J. Reina-Tosina, D. Naranjo-Hernandez, and L. M. Roa, "Measurement issues in galvanic intrabody communication: Influence of experimental setup," *IEEE Trans. Biomed. Eng.*, vol. 62, no. 11, pp. 2724–2732, Nov. 2015.
[23] W. J. Tomlinson, K. R. Chowdhury, and C. Yu, "Galvanic coupling intra-body communication link for real-time channel assessment," in *Proc. IEEE Conf. Comput. Commun. Workshops (INFOCOM WKSHPS)*, Apr. 2016, pp. 968–969.
[24] A. Vizziello, P. Savazzi, G. Magenes, and P. Gamba, "PHY design and implementation of a galvanic coupling testbed for intra-body communication links," *IEEE Access*, vol. 8, pp. 184585–184597, 2020.
[25] S. Banou, M. Swaminathan, G. R. Muns, D. Duong, F. Kulsoom, P. Savazzi, A. Vizziello, and K. R. Chowdhury, "Beamforming galvanic coupling signals for IoMT implant-to-relay communication," *IEEE Sensors J.*, vol. 19, no. 19, pp. 8487–8501, Oct. 2019.
[26] A. Lay-Ekuakille, G. Griffo, P. Vergallo, A. Massaro, F. Spano, and G. Gigli, "Implantable neurorecording sensing system: Wireless transmission of measurements," *IEEE Sensors J.*, vol. 15, no. 5, pp. 2603–2613, May 2015.
[27] W. K. Chen, Z. L. Wei, Y. M. Gao, Z. L. Vasic, M. Cifrek, M. I. Vai, M. Du, and S. H. Pun, "Design of galvanic coupling intra-body communication transceiver using direct sequence spread spectrum technology," *IEEE Access*, vol. 8, pp. 84123–84133, 2020.
[28] T. Kang, S. Kim, K.-I. Oh, J.-H. Hwang, J. Lee, H. Park, K. Byun, and W. Lee, "Evaluation of human body characteristics for electric signal transmission based on measured body impulse response," *IEEE Trans. Instrum. Meas.*, vol. 69, no. 9, pp. 6399–6411, Sep. 2020.
[29] M. Tudela-Pi, L. Becerra-Fajardo, A. Garcia-Moreno, J. Minguillon, and A. Ivorra, "Power transfer by volume conduction: *In vitro* validated analytical models predict DC powers above 1 mW in injectable implants," *IEEE Access*, vol. 8, pp. 37808–37820, 2020.

REZA NOORMOHAMMADI received the B.Sc. degree in electrical engineering from the K. N. Toosi University of Technology (KNTU), Tehran, Iran, in 2015, and the M.Sc. degree in telecommunication engineering from the Amirkabir University of Technology (AUT), Tehran, in 2018. He is currently pursuing the Ph.D. degree with the Department of Electronic Systems, Norwegian University of Science and Technology (NTNU), Trondheim, Norway. His current research interest includes the design and development of biomedical implants communications based on electromagnetic waves.

ALI KHALEGHI (Senior Member, IEEE) received the Ph.D. degree in physics from the University of Paris XI, Paris, France, in 2006. He held a postdoctoral position at the Institute d' Electronique et de Télécommunications de Rennes (IETR), France, from 2006 to 2007, and the Intervention Center (IVS), Oslo University Hospital, Norway, from 2008 to 2009. From 2010 to 2015, he was an Assistant Professor with the Department of Electrical and Computer Engineering, K. N. Toosi University of Technology (KNTU), Tehran, Iran. He obtained several research and industrial grants during his career at KNTU. He established the Wireless Terminal Test Lab (WTT) at KNTU. He distinguished as the Best Researcher of KNTU in 2013. Since 2015, he has been a Senior Scientist with the Norwegian University of Science and Technology (NTNU) and Oslo University Hospital. He has authored over 95 journal and full conference papers and holds five international patents. His research interests include the antennas and waves propagation, wireless communications, electromagnetic compatibility (EMC), measurement techniques, and bio-electromagnetics.

ILANGKO BALASINGHAM (Senior Member, IEEE) received the M.Sc. and Ph.D. degrees from the Department of Electronics and Telecommunications, Norwegian University of Science and Technology (NTNU), Trondheim, Norway, in 1993 and 1998, respectively, both in signal processing. He performed the master's degree thesis at the Department of Electrical and Computer Engineering, University of California at Santa Barbara, USA. From 1998 to 2002, he worked as a Research Engineer for developing image and video streaming solutions for mobile handheld devices at Fast Search and Transfer ASA, Oslo, Norway, which is now part of Microsoft Inc. Since 2002, he has been with the Intervention Center, Oslo University Hospital, Oslo, as a Senior Research Scientist, where he heads the Wireless Sensor Network Research Group. He was appointed as a Professor of signal processing in medical applications at NTNU, in 2006. From 2016 to 2017, he was a Professor by courtesy at the Frontier Institute, Nagoya Institute of Technology, Japan. His research interests include super robust short-range communications for both in-body and on-body sensors, body area sensor networks, microwave short-range sensing of vital signs, short-range localization and tracking mobile sensors, and nanoscale communication networks. He has authored or coauthored over 225 journal and conference papers, seven book chapters, 42 abstracts, six patents, and 20 articles in popular press. He has given 16 invited/ keynotes at the international conferences. In addition, he is active in organizing conferences, including the Steering Committee Member of ACM NANOCOM for term 2018–2021, the General Chair of the 2019 IEEE International Symposium of Medical ICT and the 2012 Body Area Networks (BODYNETS) conference, and the TPC Chair of the 2015 ACM NANOCOM. He was an Area Editor of *Nano Communication Networks* (Elsevier) in 2013.